Accelerator Division
Alternating Gradient Synchrotron Department
BROOKHAVEN NATIONAL LABORATORY
Upton, New York 11973

Accelerator Division
Technical Note

AGS/AD/Tech. Note No. 386

A FAST ENVELOPE DETECTOR

by

D. Ciardullo

December 29, 1993

A FAST ENVELOPE DETECTOR

INTRODUCTION

Traditional AM demodulating methods include both synchronous (product detector) and non-synchronous (rectification) techniques. While each has its merits, both methods require some amount of filtering to accomplish their goal of envelope detection. In certain applications (for example, when the detection scheme is utilized within a feedback loop), the resulting circuit delays present severe limitations to the system's response time. This paper describes a wideband, active envelope detector with a response time on the order of 1µsec. The circuit described has a demodulation bandwidth of DC≈350kHz, and provides a high degree of linearity over a dynamic range in excess of 40dB. The device is designed for broadband carrier operation (1MHz to 5MHz), but can easily be adapted to demodulate carriers in other ranges (up to VHF).

The circuit described was developed to provide a real-time monitor for an amplitude modulated rf signal swept in frequency from 1MHz to 5MHz. Although the specific accuracy, linearity and dynamic range requirements could have been satisfied using more conventional detector techniques, its inclusion as part of a feedback loop within a larger system was the ultimate motivation for developing this circuit. Standard average envelope detectors generally utilize a signal rectification/ filtering combination which requires a time constant much greater than one rf period (at the lowest carrier frequency) to maintain reasonable amplitude accuracy.

Most product (or synchronous) detectors use a non-linear detection scheme which requires filtering to extract the "DC" term from its output to obtain the original modulation waveform. Like the rectifier approach, this filtering adds significant delay to the response time of the detector; This technique was therefore determined unsuitable for our particular application.

To circumvent the problem of response delay, a vector addition technique is used to convert an rf sinusoid directly into a "DC" modulation signal, with minimal rf processing of the carrier. This method is easily implemented using currently available high speed analog transconductance multipliers. It achieves amplitude demodulation at frequencies approaching that of the carrier, without the long time constants typical of other detection methods.

BASIC THEORY

Since minimizing delay is a primary concern, it is desired to use a detection method which does not depend on low pass filtering to extract the modulation signal. To do this, we will first split the modulated carrier into two equal parts, each of which still contains both the intelligence signal and the carrier rf. These elements may then be combined in such a manner as to null out the

rf while leaving the modulation waveform intact. The trigonometric identity

$$Sin^2(\omega t) + Cos^2(\omega t) = 1 \qquad (1)$$

shows that it is indeed possible to accomplished this task if the two components are made to be 90° apart in phase. The functional block diagram of such a detection technique is shown in Figure 1.

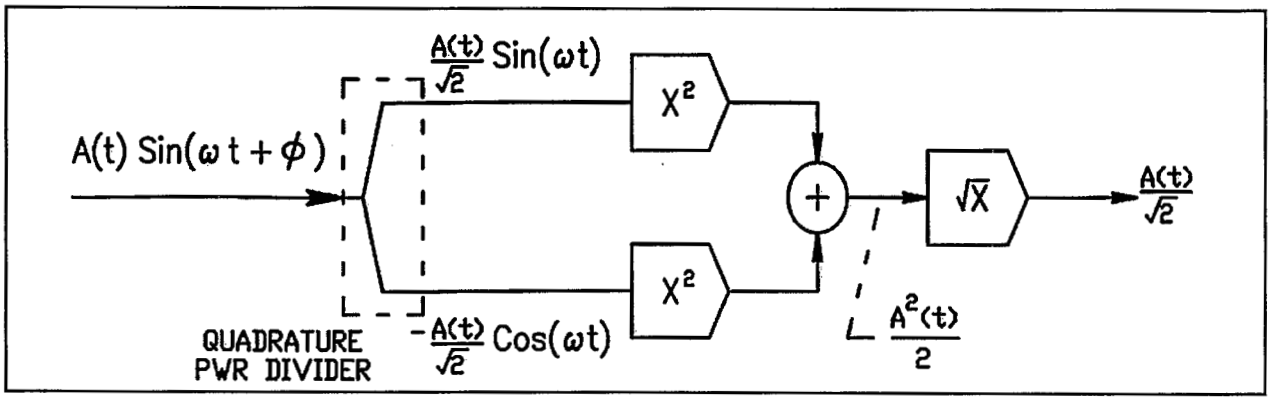

Figure 1. Envelope Detector Functional Block Diagram.

An incoming rf carrier is decomposed into two equal amplitude, quadrature phase components (I and Q):

$$I\ component : \frac{A(t)}{\sqrt{2}} Sin(\omega t)$$

$$Q\ component : \frac{-A(t)}{\sqrt{2}} Cos(\omega t) \qquad (2)$$

where A(t) is the amplitude of the carrier as a function of time (i.e., the modulation waveform) and w is the carrier frequency. Note that we have assumed here the use of a power divider to obtain the quadrature phase split, with some insertion phase ϕ (which is dependent upon the rf frequency). The vector sum of the two components is explicitly carried out to obtain a linearly scaled version of the amplitude modulating function, A(t).

To obtain the vector sum, both components of the original carrier are squared, then added together. The square root of "the sum of the squares" is then computed real-time to obtain:

$$\sqrt{[\frac{A(t)}{\sqrt{2}}]^2 Sin^2(\omega t) + [\frac{-A(t)}{\sqrt{2}}]^2 Cos^2(\omega t)} = \frac{A(t)}{\sqrt{2}} \qquad (3)$$

using the trigonometric identity of equation 1. An important consequence of this result is the fact that there is no rf term in

the solution; Although we started out with two rf (amplitude modulated) sinusoids, the result is a scaled version of the modulation waveform *only*. The significance of this outcome is two-fold; First, even though two non-linear operations were involved, no filtering is required to separate the carrier from the original modulation waveform. Since no filtering is required, there are no long time constants to slow down the overall detector's response time. In addition, the modulation frequency can approach the actual carrier rf, since there is no need to allow room for filter "skirts". The second implication of this result is one of practicality; Any analog processing which follows this portion of the electronics need only operate at the modulation frequency (as opposed to at rf). Time delay and slew rate now become the chief design considerations from this point on in the circuit, rather than rf bandwidth.

IMPLEMENTING THE BLOCK DIAGRAM

A schematic for the Envelope Detector constructed is shown in Figure 2. The drawing is divided into three basic sections; Vector Decomposition, Vector Magnitude Computation and post processing gain/offset/distribution. Amplifier U1 is used to scale the maximum amplitude of the modulated rf to $2V_{pp}$. This upper limit is a constraint imposed by the maximum input voltage to the *Vector Magnitude* section (the *Vector Decomposition* section has unity gain). Potentiometer R1 is calibrated such that the peak carrier voltage applied to the input of the circuit results in $\pm 1V_{pk}$ at the output of U1. This adjustment matches the input signal to the AD834s to make full use of their dynamic range.

Quadrature Phase Division

The 90° phase split can be accomplished using a good quality quadrature power divider, many of which are available commercially. Using such a device provides a quick, easy solution for frequencies above approximately 100kHz, particularly if wideband carrier reception is not a main concern. Active all-pass networks [1] are a good choice for carriers in the HF frequency range and below, especially for applications where a 90° splitter doesn't exist "off the shelf" or when its cost is prohibitively expensive. The advantage to using an active all-pass network as opposed to a passive one is the amplitude match afforded by using operational amplifiers. The use of feedback provides a very flat amplitude response, resulting in a broadband amplitude balance between quadrature outputs that is difficult to match using passive networks. An active phase split also provides gain to preserve the original amplitude of the input signal, eliminating the $1/\sqrt{2}$ scaling factor associated with a power divider. Broader band operation can be accomplished by simply cascading additional sections, without incurring an appreciable loss in carrier signal or a significant increase in amplitude ripple.

The decision of which 90° phase shifting technique to use was based upon amplitude balance, cost and frequency range requirements. For the detector circuit shown in Figure 2, AD847 high speed OP-AMPs are used to realize a pair of three section active all-pass networks, which provide quadrature outputs over a frequency range of 1 MHz - 5 MHz. The AD847 is a voltage feedback

operational amplifier, selected for its high speed at unity gain, as well as its amplitude and phase characteristics at the carrier frequencies of interest. Figure 3 shows the absolute amplitude response of both quadrature outputs. The constant level shift between the two plots is primarily due to the non-exact component value match of the resistors used for reverse termination of each output. Note the response flatness out to just above 3 MHz, where the plots begin a slight roll off. Though down by only 0.3dB at 5MHz, this translates directly into a 0.3dB amplitude error for the overall detector. The vector sum circuitry cannot distinguish between a change in amplitude at the input to the detector or changes in the response characteristic of the quadrature splitter. For this reason, it is important to minimize both the absolute response ripple *and* the relative amplitude imbalance between outputs of the splitter within the desired band of operation, especially if the envelope detector is to be used in a high accuracy application.

The relative amplitude imbalance and deviation from quadrature phase for the active splitter outputs is shown in Figure 4. The worst-case phase deviation is ≈1.7° at 1 MHz, the low end of the frequency band of interest. In general, deviations from 90° of a few percent will have minimal effect on the vector sum **[2,3]** (and hence on the overall envelope detection error).

Implementing The "Sum of Squares" Function

The next step in implementing the block diagram of Figure 1 involves squaring each of the quadrature modulated carriers. It is desirable to use variable transconductance type multipliers (as opposed to rf mixers) to carry out this function, to eliminate any need for filtering unwanted harmonics at the output. Each carrier is applied to both inputs of its associated multiplier. The resulting outputs are then

$$[A(t)\,Sin(\omega t)]^2 = \frac{[A(t)]^2}{2}[1 - Cos(2\omega t)]$$

$$[-A(t)\,Cos(\omega t)]^2 = \frac{[A(t)]^2}{2}[1 + Cos(2\omega t)] \qquad (4)$$

where the modulation function A(t) is greater by a factor of √2 than in Equation [3]; This is a consequence of using an active 90° phase split as opposed to a power divider. As can be seen by Equation [4], the multiplier chosen should be capable of operating at twice the carrier frequency. In addition it should be a four-quadrant device, since both inputs must be capable of accommodating a bipolar signal.

The Analog Devices AD834 transconductance multiplier was selected for this application due to its excellent combination of accuracy, dynamic range and DC to 500 MHz bandwidth. The AD834 also has differential current outputs which can be parallelled with one or more similar devices, providing a convenient method of summing their outputs. Since current addition is inherently wideband, use of these multipliers eliminates the need for an additional DC-

coupled broadband summing device. Adding the outputs from both AD834s we obtain

$$408mV\left[\frac{[A(t)]^2}{2}[1 - Cos(2\omega t)] + \frac{[A(t)]^2}{2}[1 + Cos(2\omega t)]\right] = 408mV[A(t)]^2 \quad (5)$$

where the 408mV scaling factor is a result of the ±4mA output current of the AD834 (from its transfer function) through 51Ω resistors R66 and R67 in the schematic of Figure 2.

The differential nature of the AD834 outputs requires the use of a difference amplifier (e.g. an OP-AMP or an instrumentation amplifier) to convert the "sum of squares" into a single-ended voltage. The amplifier chosen for this purpose need not be capable of operation at the rf frequency; Equation [5] illustrates that once the squares of the quadrature carriers are added together, all that remains is a scaled version of the square of the modulation term, devoid of any rf. Selection of an appropriate differential amplifier depends upon the delay and common mode input voltage handling of the amplifier, as well as on the slew rate and bandwidth of the modulation. As indicated in the circuit schematic of Figure 2, an Analog Devices AD847 operational amplifier was chosen for this task.

Inspection of the circuit schematic in Figure 2 reveals that each AD834 is configured to output the negative of the square of its input. This is done as a practical matter to reduce crosstalk between the input and output pins. Since the same technique is applied to all three devices which contribute differential current to the summing node, only the sign of the final result is affected. The reader is directed to references **[5]** and **[6]** for information regarding the practical aspects of circuit design with the AD834 multiplier.

Implementing The Square Root Function

To complete the analog vector sum computation (and hence reconstruct the modulating waveform A(t)), it is necessary to take the square root of the result found in Equation [5]. Several analog computational ICs capable of performing this calculation are available commercially. One should note, however, that this computational step presents significant limits on both the dynamic range and time delay specifications for the overall envelope detector. For example, a 40dB dynamic range at the output of the square-root function (the output of the detector) necessitates an 80dB range at its input. In addition, the device selected needs to have sufficient bandwidth to accommodate both the expected modulation frequency and the overall delay specifications for the circuit.

For the envelope detector constructed, a squarer is placed in the feedback loop of an operational amplifier to approximate the square root function shown in Figure 1 **[4]**. This particular computational method was selected because it allows us to further capitalize on the benefits of the current summing technique used to implement the "sum of squares" in Equation [5]. In this case, a third AD834 multiplier operates as the squaring device. The output

of the third AD834 is simply parallelled with the outputs from the two previous multipliers, but with its two output pins reversed. This has the effect of subtracting the differential output current of the third AD834 from the sum of the other two. [Note, however, that the common mode currents of all three multipliers still add]. The difference voltage across the summing node is amplified by the full open loop gain of the AD847 operational amplifier, which changes its output voltage until the voltage at both its inputs are equal (i.e., the differential summing node nulls to zero). A simplified block diagram representation of this feedback loop is illustrated in Figure 5. This diagram is meant as a generalized illustration of the envelope detector. As such, the scaling details of the AD834s used to effect the squaring function blocks have been left out for clarity. [It can be seen from the schematic of Figure 2 that each multiplier is actually configured to output a scaled version of the negative square of its input].

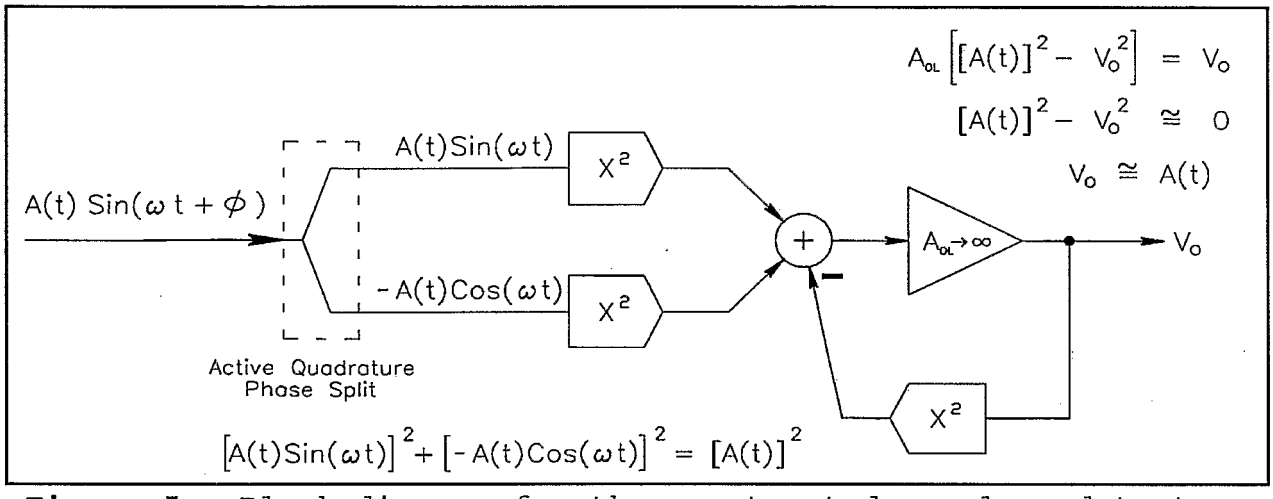

Figure 5. Block diagram for the constructed envelope detector.

As shown in the diagram, the output of the summing junction is multiplied by the open loop gain of the amplifier, resulting in

$$A_{OL}\,[\,[A(t)\,Sin(\omega t)]^2 + [-A(t)\,Cos(\omega t)]^2 - V_o^2\,] = V_o \qquad (6)$$

If the open loop gain is assumed to be large (A_{OL}≈70 dB for the AD847), then

$$[A(t)\,Sin(\omega t)]^2 + [-A(t)\,Cos(\omega t)]^2 - V_o^2 \Rightarrow 0 \qquad (7)$$

where each term on the left side of the equation represents the differential output from one of the three multipliers. Substituting Equation [5] into [7] and solving for V_0 results in

$$[A(t)]^2 - V_0^2 \approx 0$$

$$V_0 \approx A(t) \qquad (8)$$

The voltage appearing at the output of the AD847 is thus "the square root of the sum of the squares", which is essentially the DC-coupled vector sum of the quadrature amplitude modulated carriers. This approximation also holds true when using the AD834s to effect the squaring functions in Figure 5; The high open loop gain of the AD847 OP-AMP is more than enough to compensate for the 0.408 scaling factor of the multipliers (±4mA full scale output into 102Ω, as compared with their ±1V input amplitude).

Other Peripheral Circuitry

One half of amplifier U15 is used to adjust the gain and offset of the detected rf (this particular adjustment is application specific). U15-U20 serve to buffer and distribute the detected rf, with each output capable of driving into a 50Ω load.

RESULTS

To evaluate the performance of the constructed envelope detector it is necessary to have some method of amplitude modulating an rf carrier. The performance of the modulator must meet or exceed that of the envelope detector if the test results are to be meaningful. For the results presented here, the device used to accomplish this task is a circuit based on the AD834 multiplier.

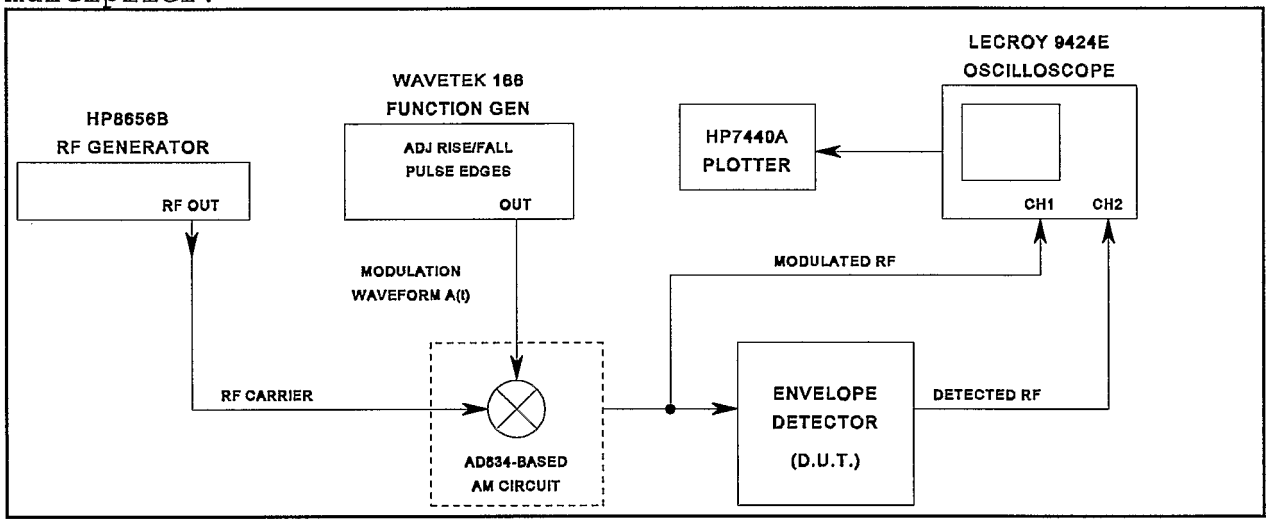

Figure 6. Test set-up for time domain performance evaluation.

Figure 6 shows the test set-up used for the time domain plots of Figures 6 and 7. The Wavetek function generator is first set to output a square pulse as the amplitude modulating function A(t) for the purpose of measuring the rise and fall times of the envelope detector. The rf source is set to output a carrier frequency of 4.5 MHz at the maximum amplitude acceptable to the modulator. Figure 7(a) shows the rise time of the envelope detector to be on the order of 1 µsec (10%-90%); The plot also indicates an additional propagation delay time from input to output of about 400 nsec. The fall time of the detector under test is shown in Figure 7(b) to be approximately 1.5 µsec.

Next, the Wavetek is set to output a triangular waveform at a

modulation frequency of 1 kHz. The amplitude of the waveform is adjusted to achieve close to 100% modulation of the carrier. Figure 8(a) shows the oscilloscope traces of both the modulated 4.5 MHz carrier and the detected rf (both traces overlay one another). Figure 8(b) is an expanded view, showing the amount of "failure to follow" distortion at low signal levels. These plots give a rough indication of the linearity and dynamic range for the detector, and can be used for initial circuit alignment. The lower bound on the dynamic range is minimized by adjusting the "zero input offset" potentiometer. Post processing gain and offset adjustments are determined by the particular application requirements for the circuit. Figures 9(a) and 9(b) are similar plots, at a modulation frequency of 10kHz.

Figure 10 illustrates the set-up used to obtain the plots in Figures 11 through 14.

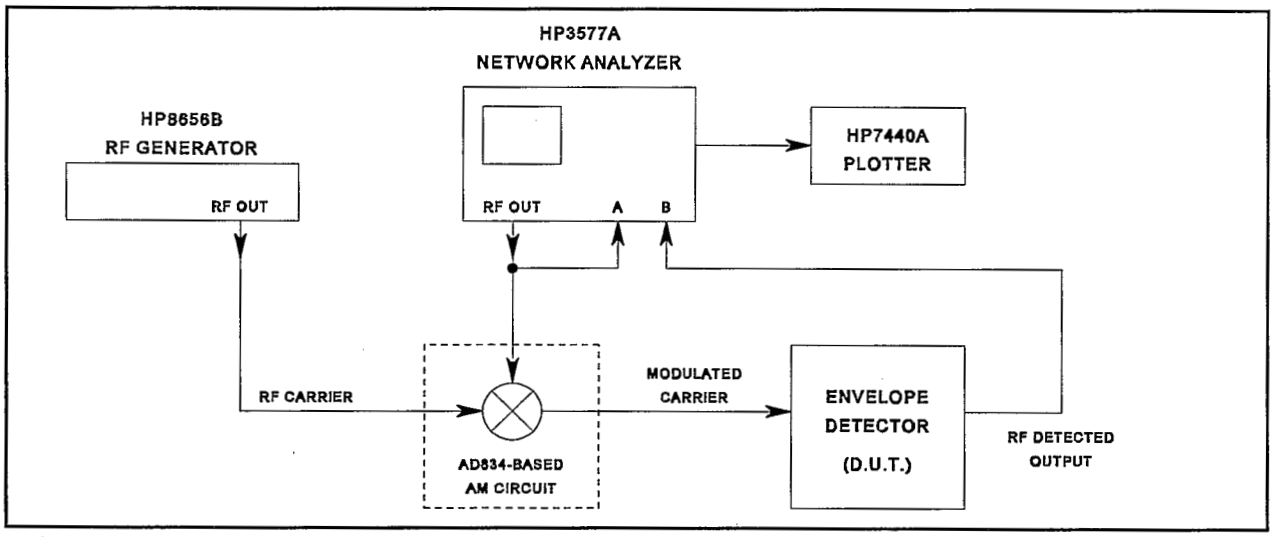

Figure 10. Test set-up for network analyzer based measurements.

For these measurements, an HP3577A network analyzer is used to modulate the rf with a swept sinusoid. The output of the envelope detector is then compared with the original modulating waveform to determine its accuracy under a variety of carrier conditions. For the tests that follow, the AD834-based modulating circuit shown in the diagram is adjusted to provide approximately 20% carrier modulation. The reader should note that the following results represent the performance of the modulator/envelope detector pair, since the modulator is in fact inside the measurement loop of the network analyzer. The delay performance of the modulator is expected to be better than that of the detector because of its 30MHz bandwidth. Amplitude accuracy and dynamic range, however, are expected to be similar, based upon these specifications for individual components utilized in the modulator circuitry.

The plot of Figure 11 shows the amplitude and phase response of the envelope detector for a single carrier frequency of f_{rf}=4.5 MHz, with the modulating signal swept from 5 Hz to 1 MHz. The top trace is the amplitude response (3dB/div), indicating a -3dB bandwidth of just below 390 kHz. A high degree of amplitude accuracy is indicated by the response flatness, which is shown to

be better than 0.5 dB (±0.25 dB) up to a modulation frequency of 100 kHz. For those applications requiring the detector to reside within a feedback loop, trace 2 is the phase response (45°/div) of the detector. The circuit exhibits 45° of phase shift at a modulation frequency of approximately 180 kHz.

Figure 12 consists of 10 individual amplitude response plots, overlaid on the same graph. The plots are intended to show the dynamic range of the detector with respect to the amplitude of the carrier signal. Each of the traces results from a 5 dB decrease in carrier amplitude. [In each case, the carrier has approximately 20% amplitude modulation]. The demodulation bandwidth does not start to significantly decrease until the carrier is approximately 35 dB down from its maximum amplitude. The detector circuit is still observed to be useable to -45 dB, but with modulation bandwidths only up to 10 kHz.

It is also desired to evaluate the envelope detector at different carrier frequencies, since the circuit constructed was designed to operate with carrier frequencies over a span of 1MHz-5MHz. The results of such a measurement are shown in Figure 13. For this test, the modulation frequency is swept from 1kHz to 100kHz. Since we are looking for small (on the order of tenths of a dB) changes, the upper modulation frequency was limited to 100kHz for the purpose of expanding the scale per division of the plot. Each trace in the figure represents a different carrier frequency, ranging from 1.0MHz to 5.0MHz in 500kHz increments. Note that the shape factor of all nine plots are similar. From the graph, carrier frequencies from 1MHz to 3MHz are clustered within 0.07 dB of one another. Significant amplitude errors begin to be observed above approximately 3MHz, a some of which can be accounted for in Figure 3 (the amplitude response of the quadrature phase split circuitry). It should be noted here that the device used to modulate the rf in the test set-up (the AD834-based modulator in Figure 10) has as part of its circuitry a low pass filter with a nominal cutoff frequency (-3dB) of 6MHz. The response roll-off of this LPF is believed to be predominantly responsible for the relatively large apparent decrease in amplitude accuracy as the carrier frequency is increased above 4.5MHz. In other words, the envelope detector is actually responding to the soft portion of the LPF's roll-off.

The final plot, presented in Figure 14, shows the delay of the circuit for various carrier frequencies. In this measurement, the modulation frequency is swept from 10Hz (the lowest frequency available from the network analyzer) to 500kHz. The upper modulation frequency and lower carrier frequency were purposely chosen to coincide. It is interesting to note that the envelope detector is capable of demodulating frequencies approaching that of the carrier; This is possible because no explicit filtering is used during the AM detection process.

CONCLUSION

An envelope detector circuit has been developed which operates over a carrier range of 1MHz to 5MHz. Specific delay time requirements prevented the use of classical rectifier or product detector techniques, which depend on low pass filtering to extract

the modulation signal. To minimize the overall response time of the envelope detector, a vector addition technique is used to null the carrier while keeping the modulation intact. The circuit presented is implemented using currently available high speed analog transconductance multipliers, and achieves amplitude demodulation at frequencies approaching that of the carrier, without the long time constants usually associated with other detection methods. The specific rf carrier bandwidth is easily modified by replacing the active all-pass section of the circuit with a 90° power divider, appropriately selected (or designed) to effect the desired overall detector amplitude accuracy.

Test results for the envelope detector constructed have been presented to evaluate the device under varying conditions of modulation frequency, carrier amplitude and carrier frequency. In addition to its μsec response time, use of the vector processing method allows the device constructed to provide accurate envelope detection over a wide dynamic range. The dynamic range of the device is measured to exceed 35dB for modulation signals up to 100 kHz (45dB for modulation below 10 kHz).

REFERENCES

1. Williams, A.B., and Taylor, F.J., *Electronic Filter Design Handbook: LC, Active, and Digital Filters,* second edition, McGraw-Hill Book Company, New York, 1988.
2. Tuckman, M., "I-Q Vector Modulator-The Ideal Control Component?," MSN & CT, May 1988, pp.105-115.
3. Ciardullo, D.J., "A High Accuracy Phase Shifter Based On A Vector Modulator," RF Design, October 1993, pp.106-114.
4. Sheingold, D.H., ed., *Nonlinear Circuits Handbook.* Norwood, MA: Analog Devices Inc., January 1976.
5. Elbert, M. and Gilbert, B., "Using the AD834 in DC to 500 MHz Applications: RMS-to-DC Conversion, Voltage-Controlled Amplifiers, and Video Switches," Analog Devices Application Note #AN-212.
6. *1992 Special Linear Reference Manual,* Analog Devices Inc.
7. Clarke, K.K., and Hess, D.T., *Communication Circuits: Analysis and Design,* Addison-Wesley Publishing Company, Reading Massachusetts, 1978.
8. Couch, L.W., *Digital and Analog Communication Systems,* second edition, Macmillan Publishing Company, New York, 1987.

ACKNOWLEDGEMENTS

The author wishes to express his appreciation to Dr. J.M. Brennan for his consultation and incitement throughout the design of this circuit, and for his review of the manuscript.

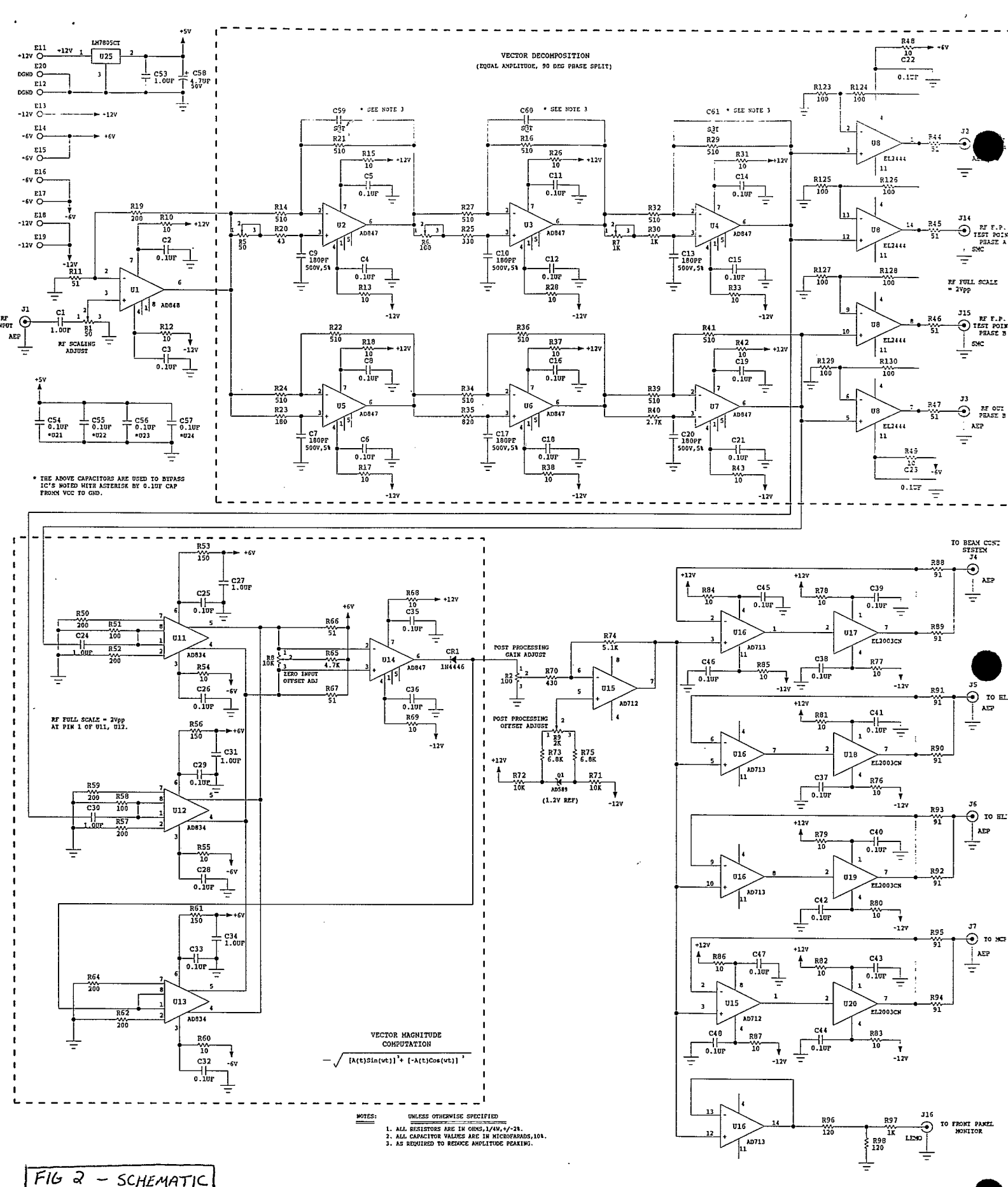

FIG 2 - SCHEMATIC

FIG 3

ABSOLUTE AMPLITUDE RESPONSE OF BOTH QUADRATURE OUTPUTS

REF LEVEL /DIV
7.710dB 0.200dB
7.710dB 0.200dB

MARKER 5 000 000.000Hz
MAG (UDF) 7.412dB

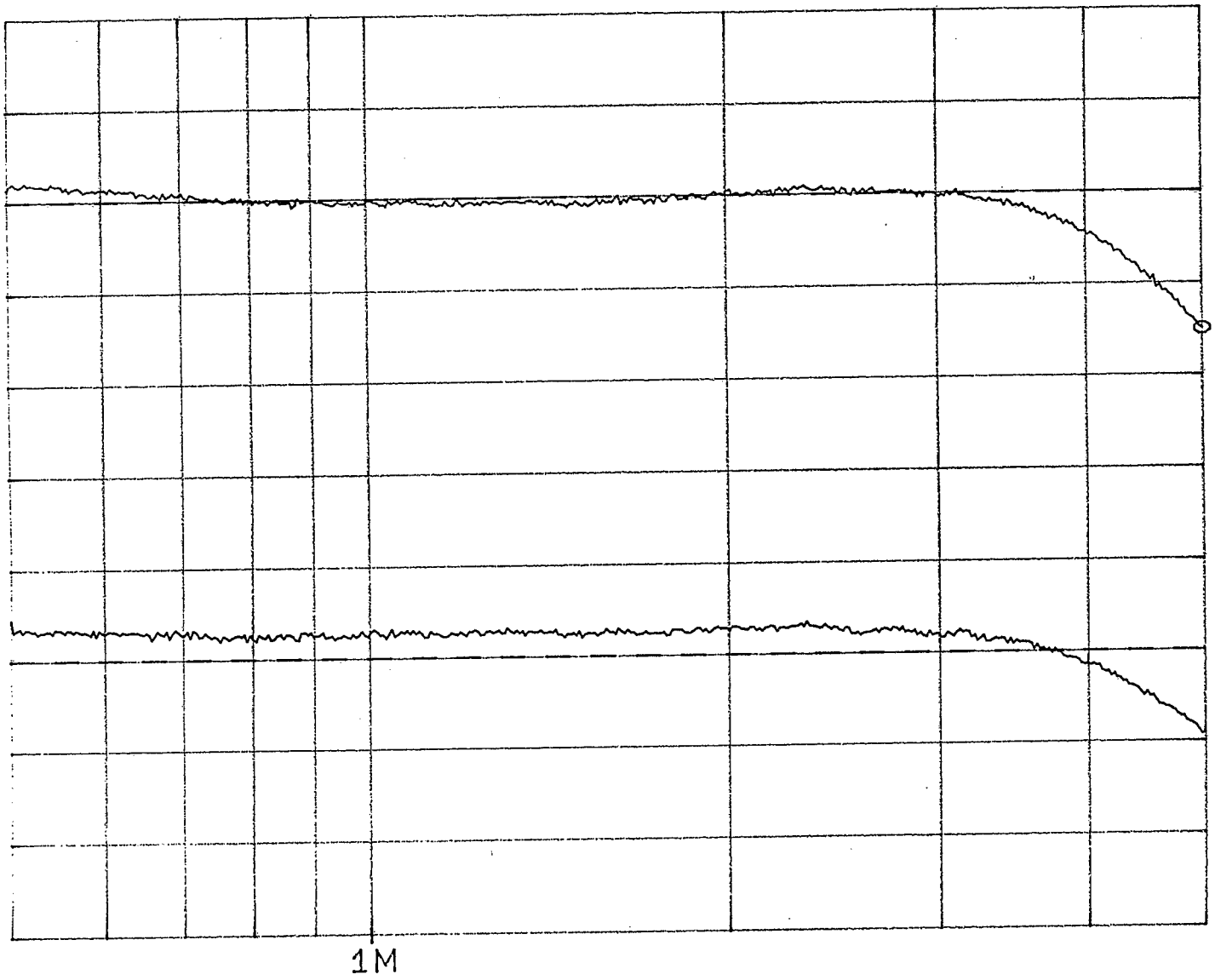

CHANNEL A
← 7.71 dB

CHANNEL B
← 7.71

START 500 000.000Hz

STOP 5 000 000.000Hz

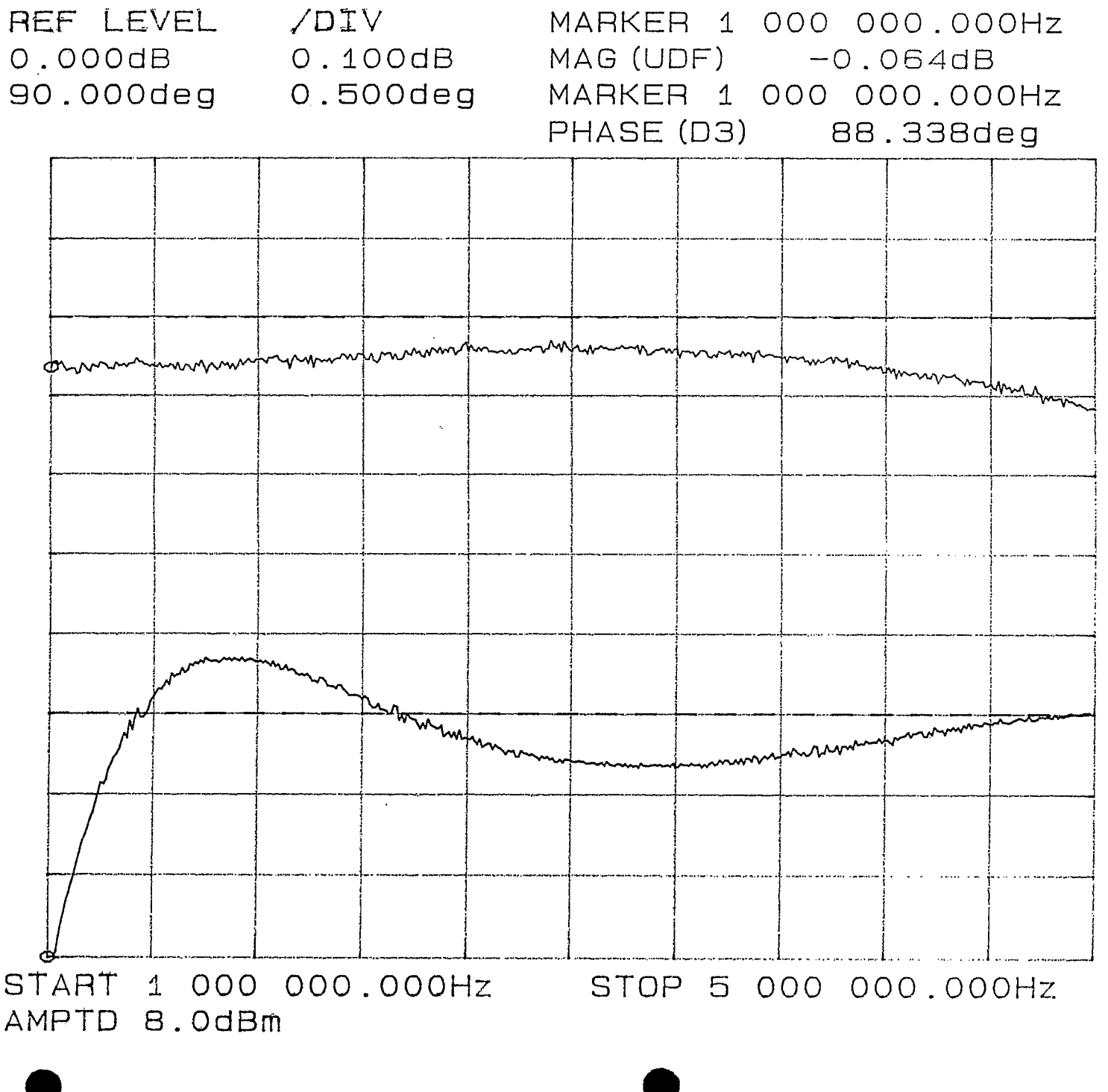

FIG 4

RELATIVE AMPLITUDE AND PHASE BALANCE OF THE TWO QUADRA OUTPUTS

AMPLITUDE BALANCE

PHASE BALANCE

MOD = 1KHz
RF = 4.5MHz

DJC 11/17/93

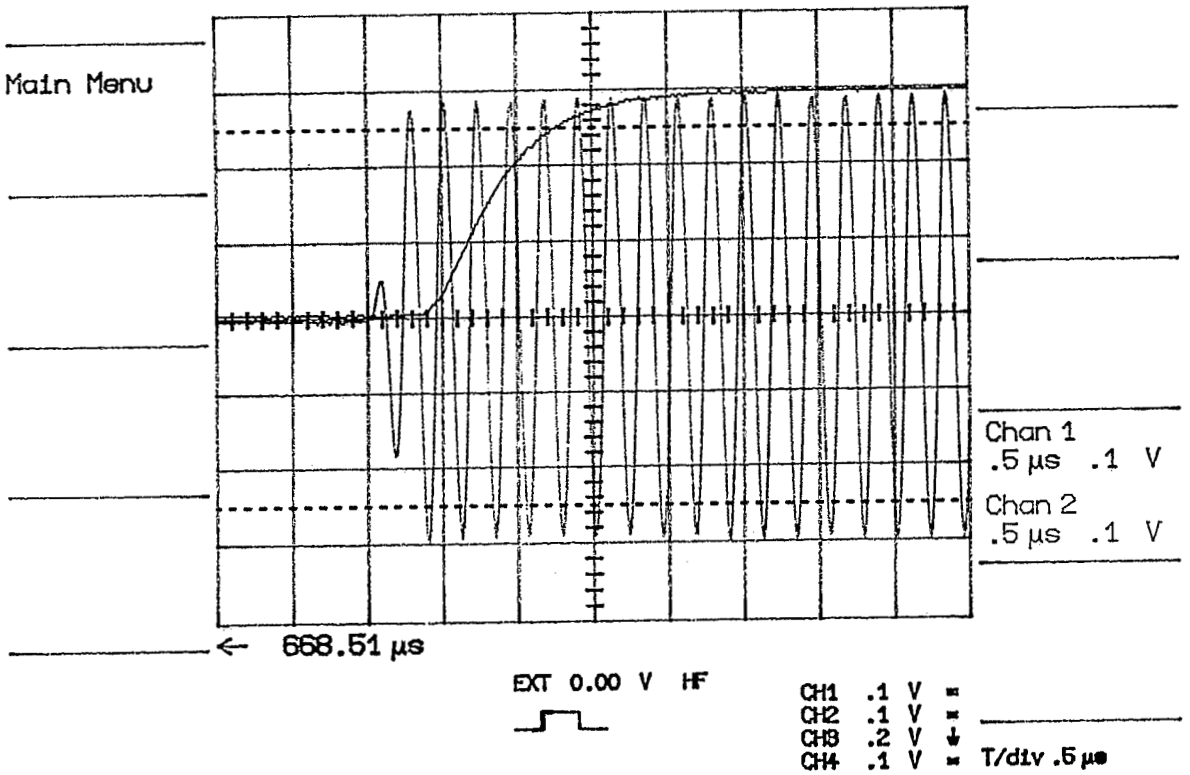

FIG 7 (a)

RISE TIME OF THE CONSTRUCTED ENVELOPE DETECTOR

FIG 7(b)

FALL TIME OF THE CONSTRUCTED ENVELOPE DETECTOR

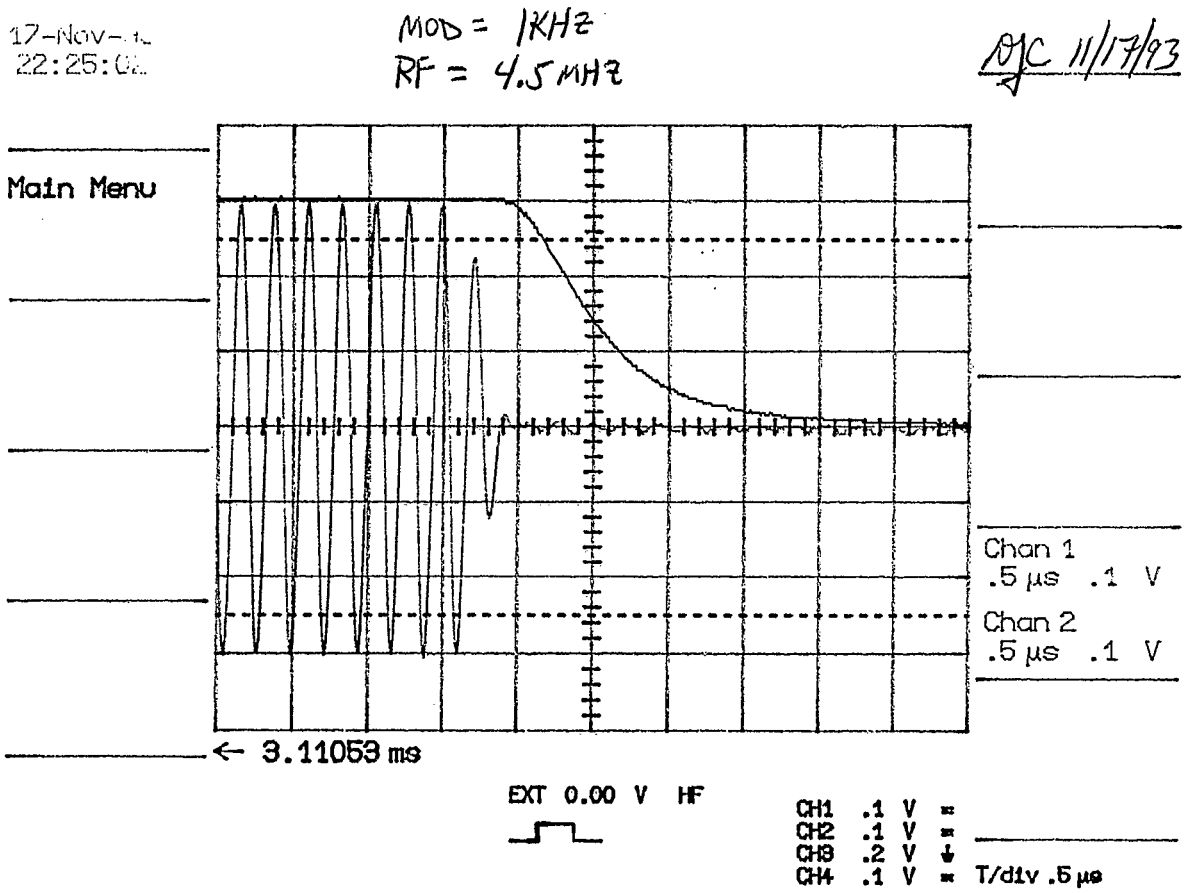

MODULATION = 1KHZ
RF = 4.5 MHZ

DJC 11/17/83

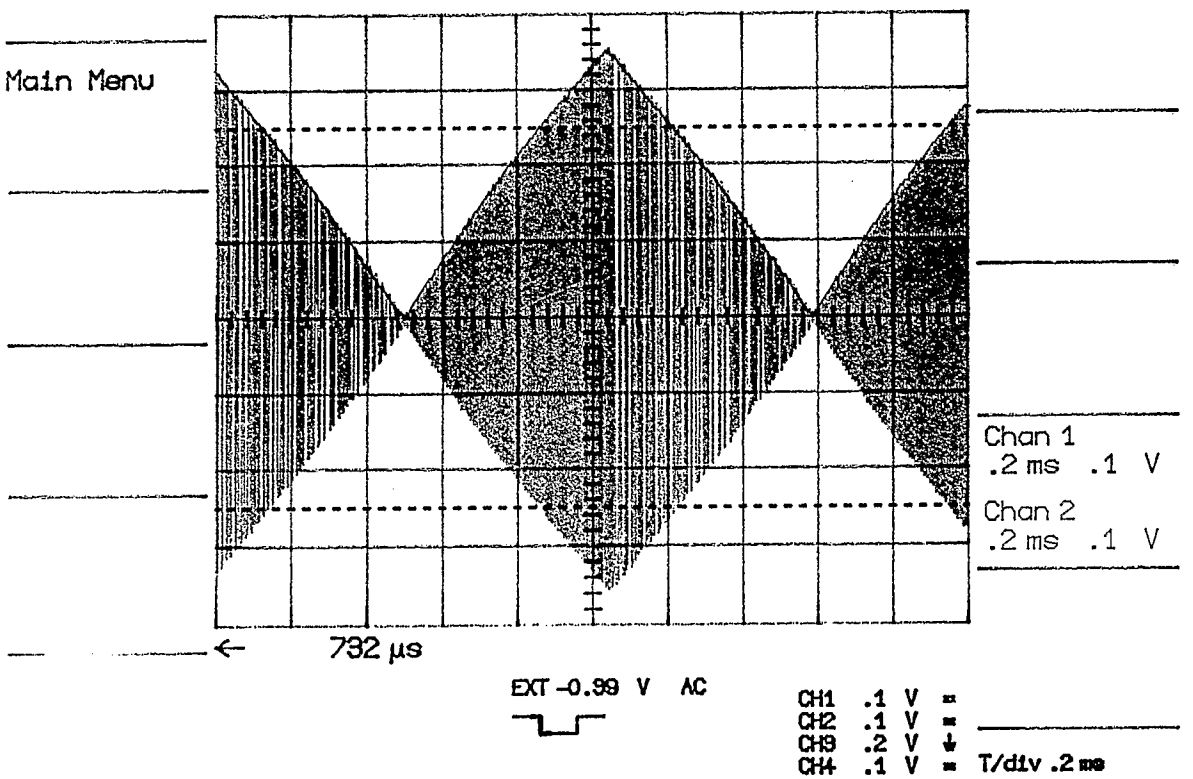

FIG 8(a)

OVERLAY OF MODULATED CARRIER AND DETECTED RF

[MODULATION FREQ = 1KHZ
RF CARRIER = 4.5MHZ]

MOD = 1 KHz
RF = 4.5 MHz

DJC 11/17/93

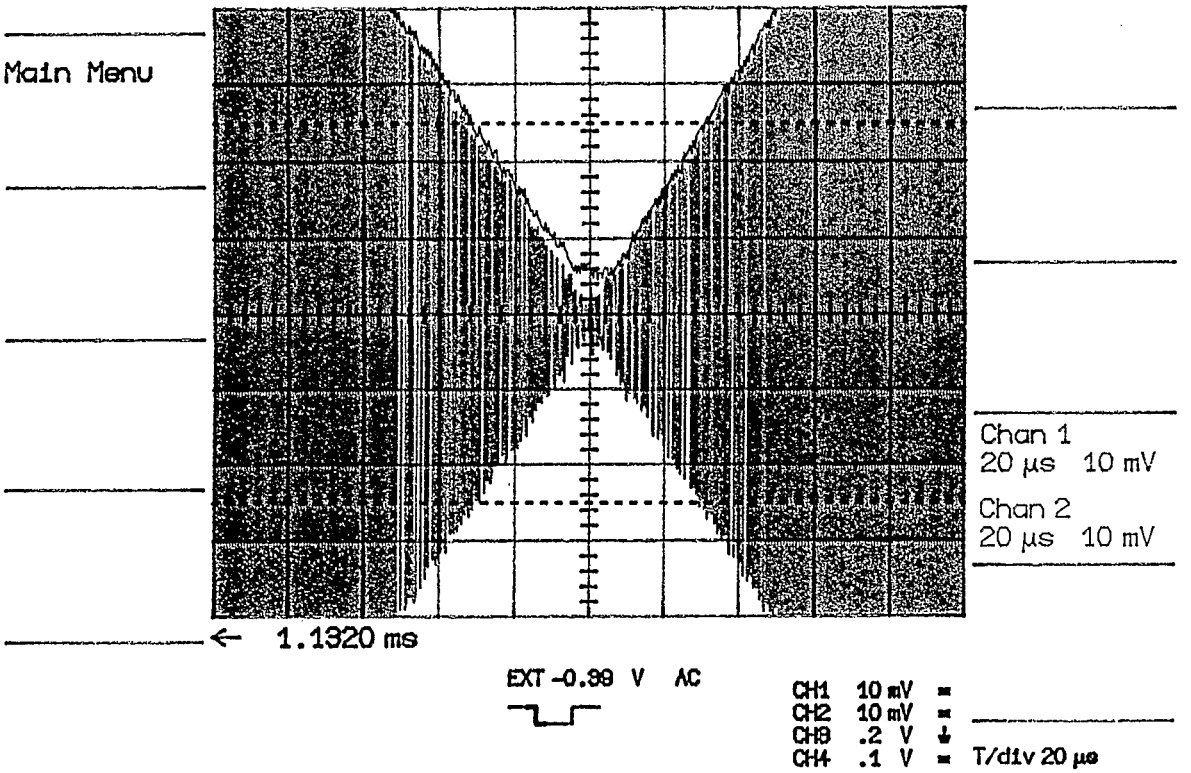

FIG 8(b)

EXPANDED VIEW OF MODULATI
CARRIER AND DETECTED RF

[MODULATION FREQ = 1 KHz
RF CARRIER = 4.5 MHz]

MODULATION = 10KHz
RF = 4.5 MHz

DJC 11/17/93

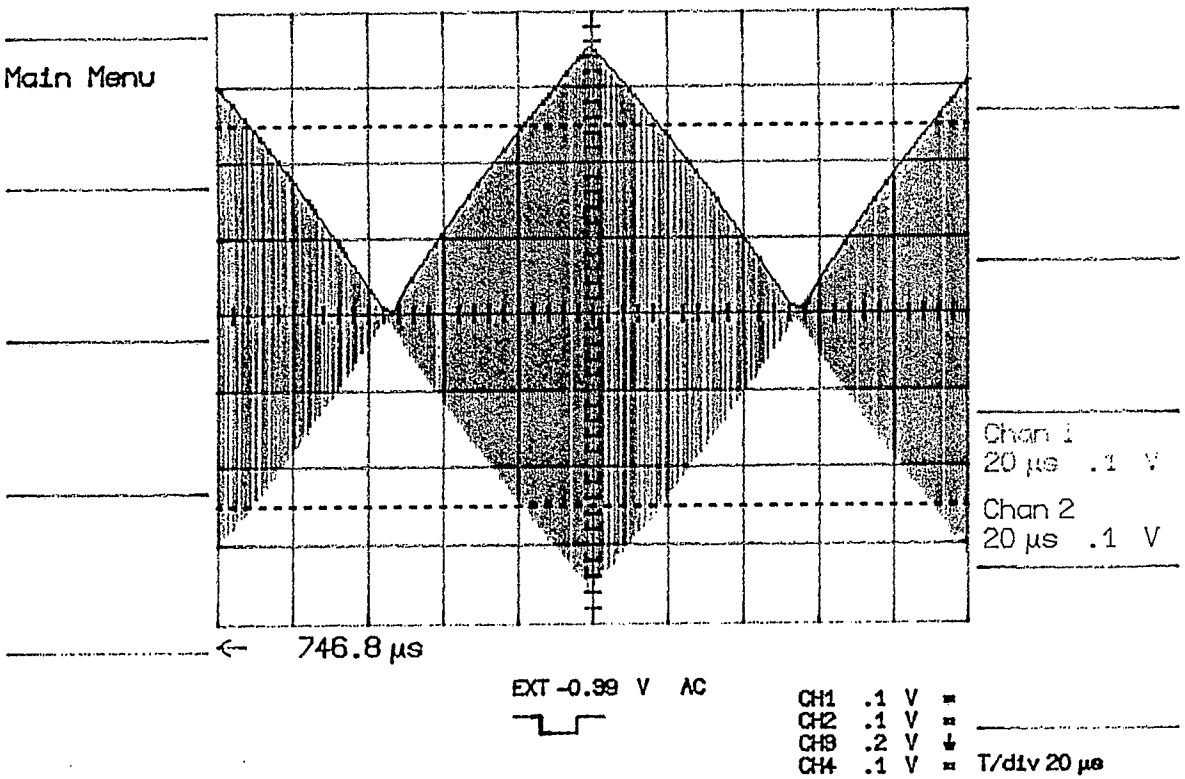

FIG 4(a)

OVERLAY OF MODULATED CARRIER AND DETECTED RF

[MODULATION FREQ = 10 KHz
RF CARRIER = 4.5 MHz]

MODULATION = 10KHz
RF = 4.5 MHz

DJC 11/17/93

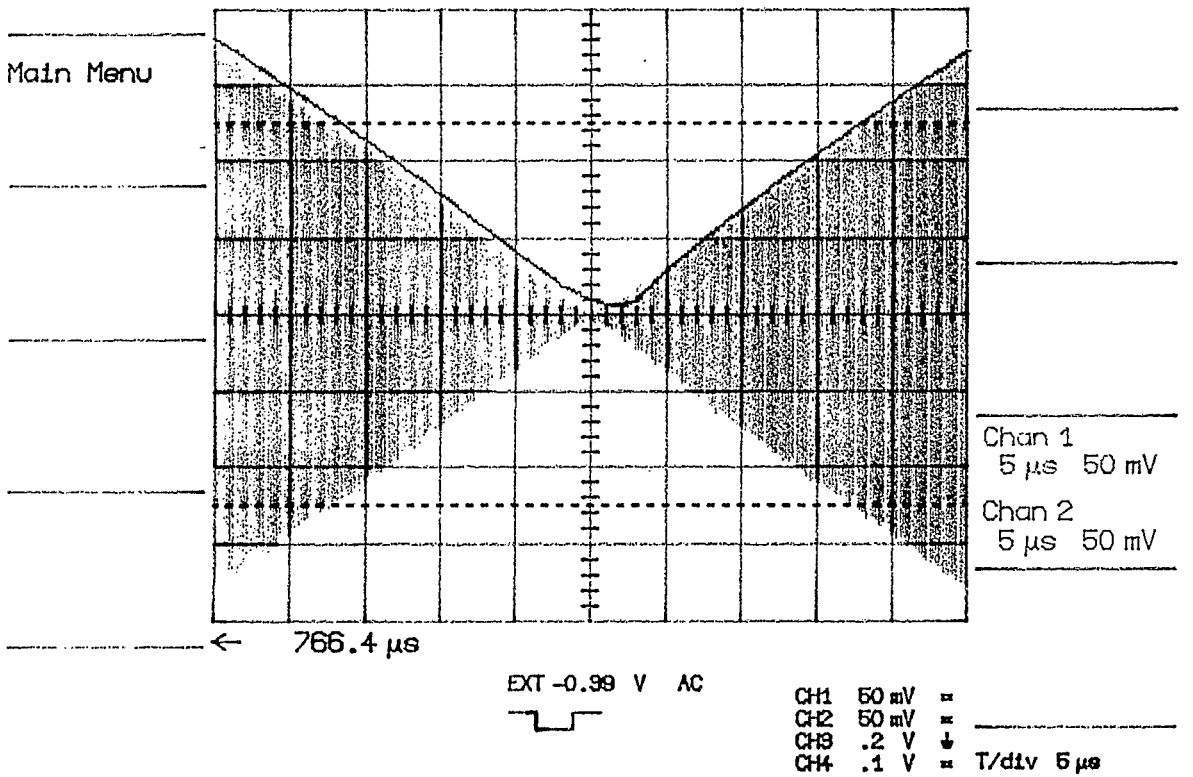

Fig 9(b)

EXPANDED VIEW OF MODULATED CARRIER AND DETECTED RF

[MODULATION FREQ = 10 KHz
RF CARRIER = 4.5 MHz]

COMPARISON OF DETECTED RF WITH MODULATION SIGNAL
(CONSTANT f_{rf} = 4.5 MHz, CONST. MOD AMPLITUDE)

REF LEVEL
-21.500dB
0.0deg

/DIV
3.000dB
45.000deg

MARKER 389 805.921Hz
MAG (UDF) -24.632dB
MARKER 183 142.879Hz
PHASE (D3) -45.315deg

FIG 11

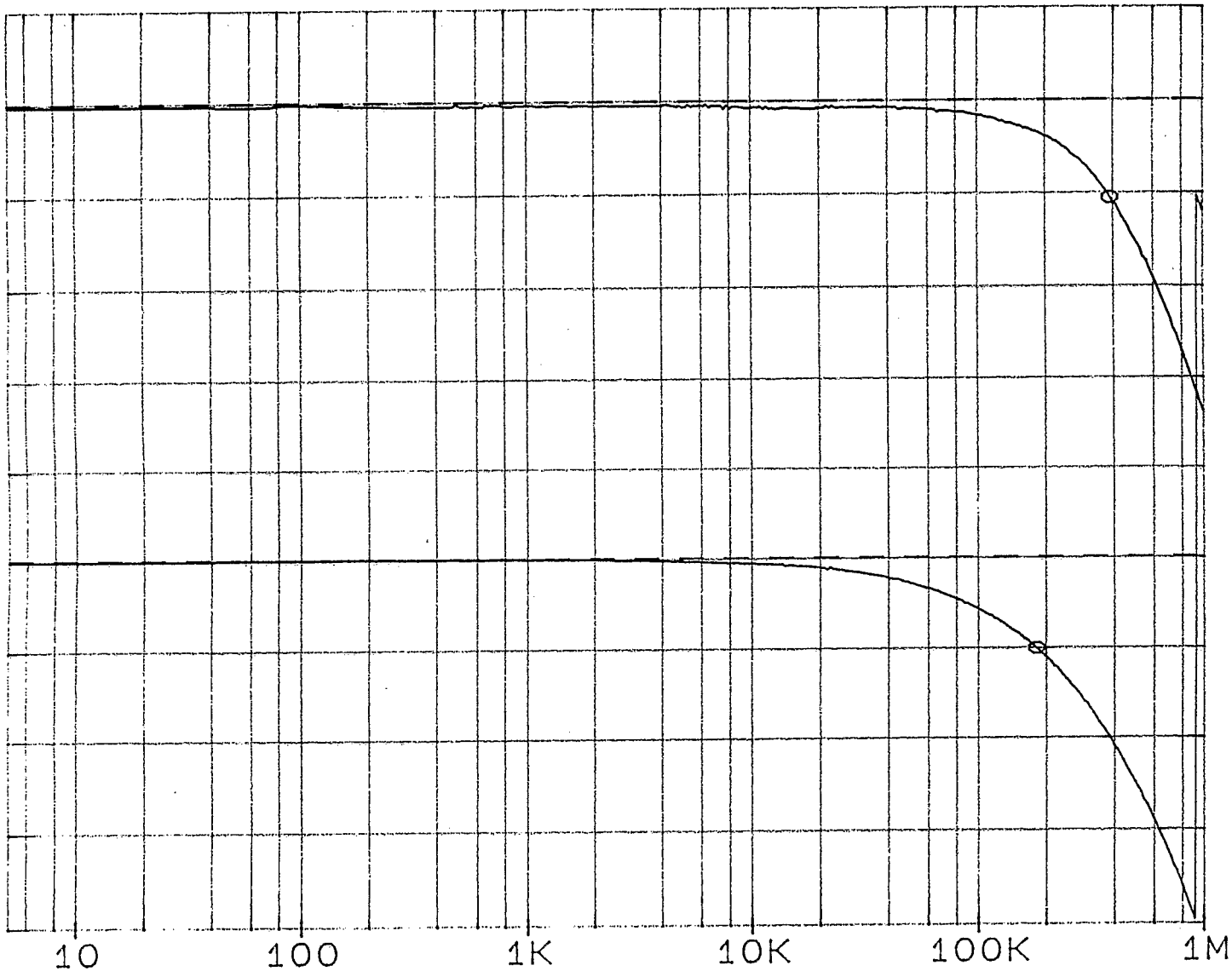

AMPLITUDE RESPONSE

PHASE RESPONSE

NJC 11/7/85

REF LEVEL /DIV
-8.250dB 5.000dB
-8.250dB 5.000dB

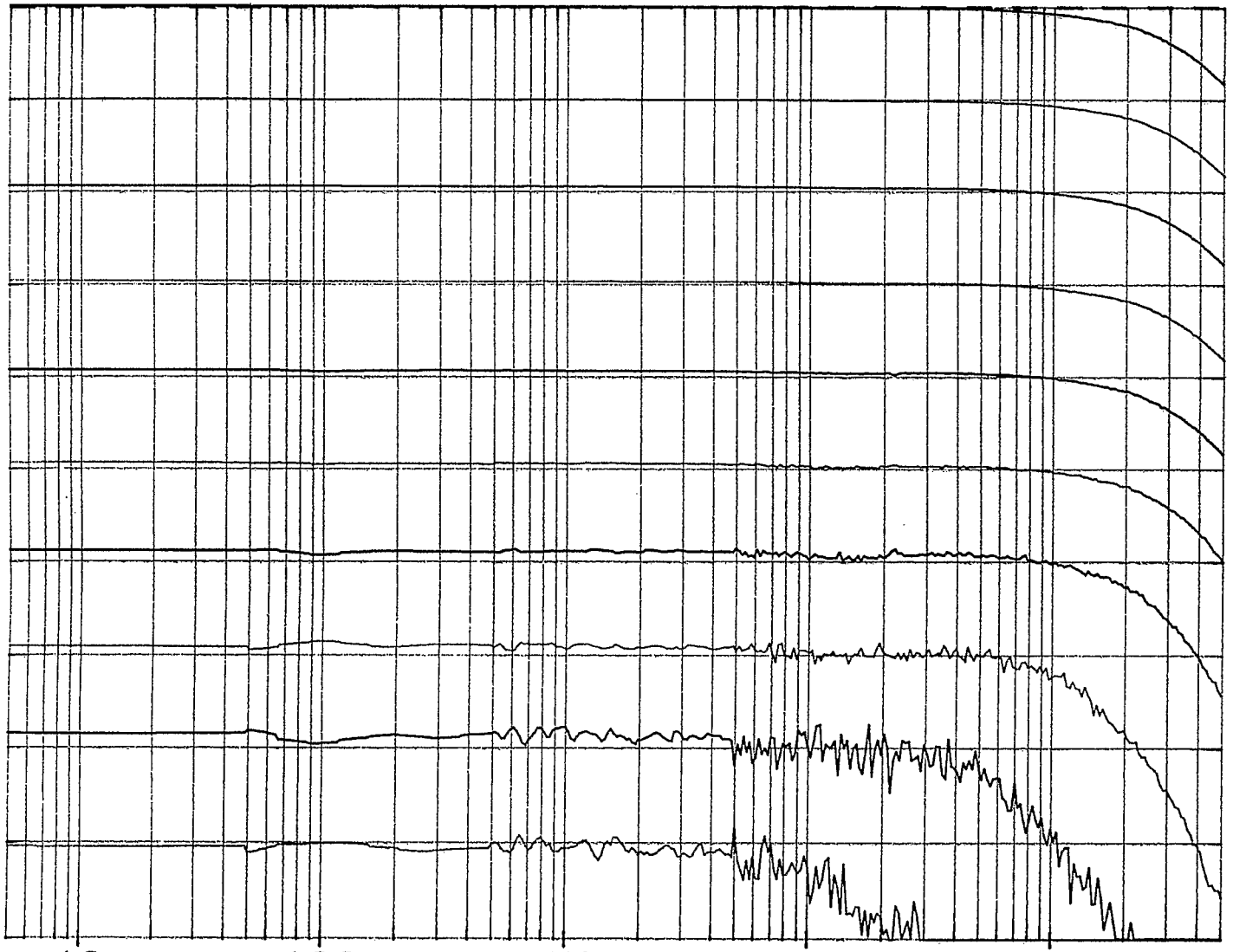

f_{rf} = 2.5MHz

R_F AMP DECREASED IN 5dB STEPS

FIG 12

DETECTED RF VS. MODULATION FREQ. FOR VARIOUS CARRIER AMPLITUDES

FOR A CONSTANT INPUT AMPLITUDE

REF LEVEL /DIV
-17.225dB 0.100dB

FIG 13

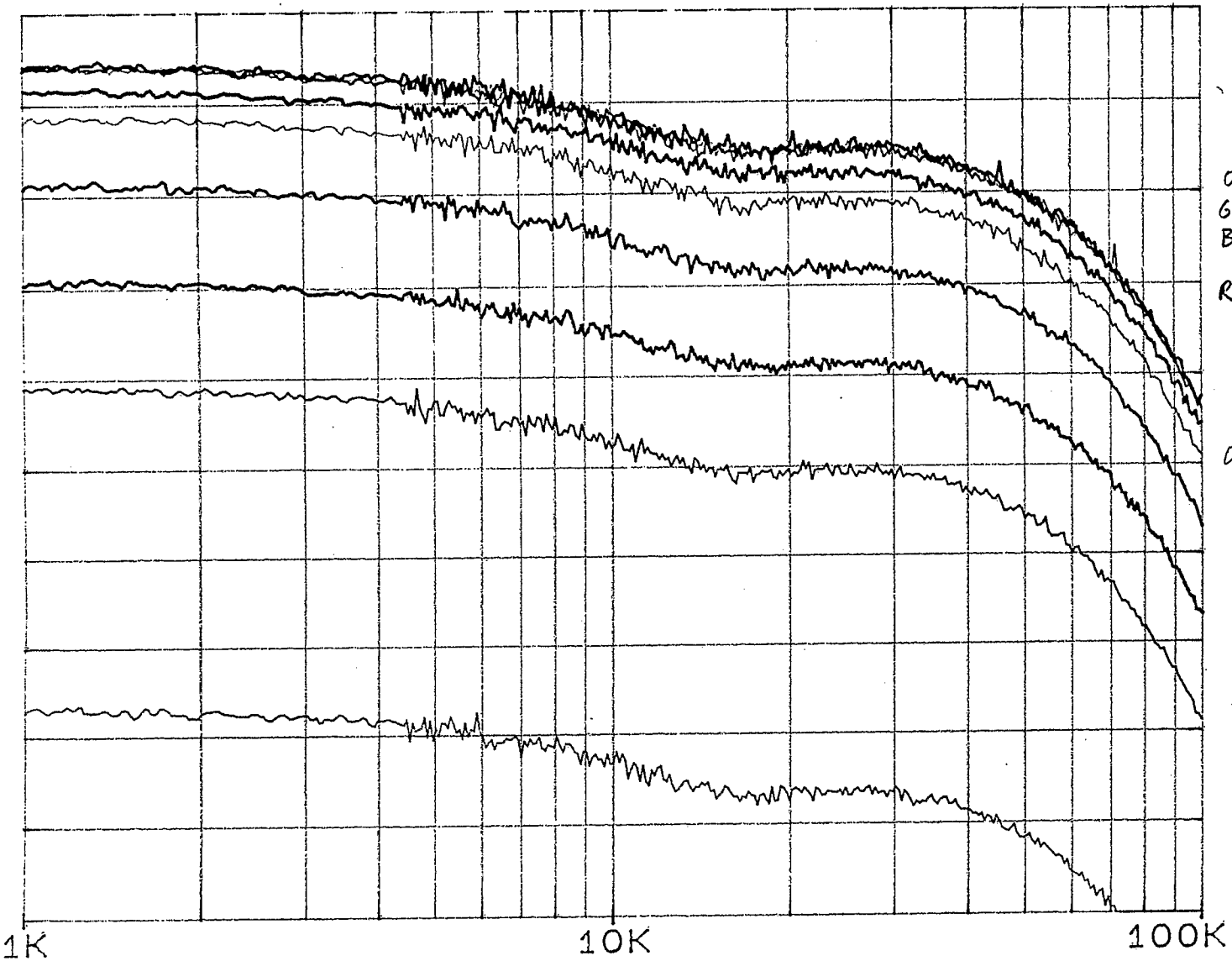

START 1 000.000Hz STOP 100 000.000Hz

NOTE: MODULATOR USED FOR TESTS HAS 5MHz LPF INSIDE

TIME DELAY, VARIOUS RF FREQUENCIES

MJC 11/9/93

REF LEVEL /DIV
500.00nSEC 100.00nSEC
500.00nSEC 100.00nSEC

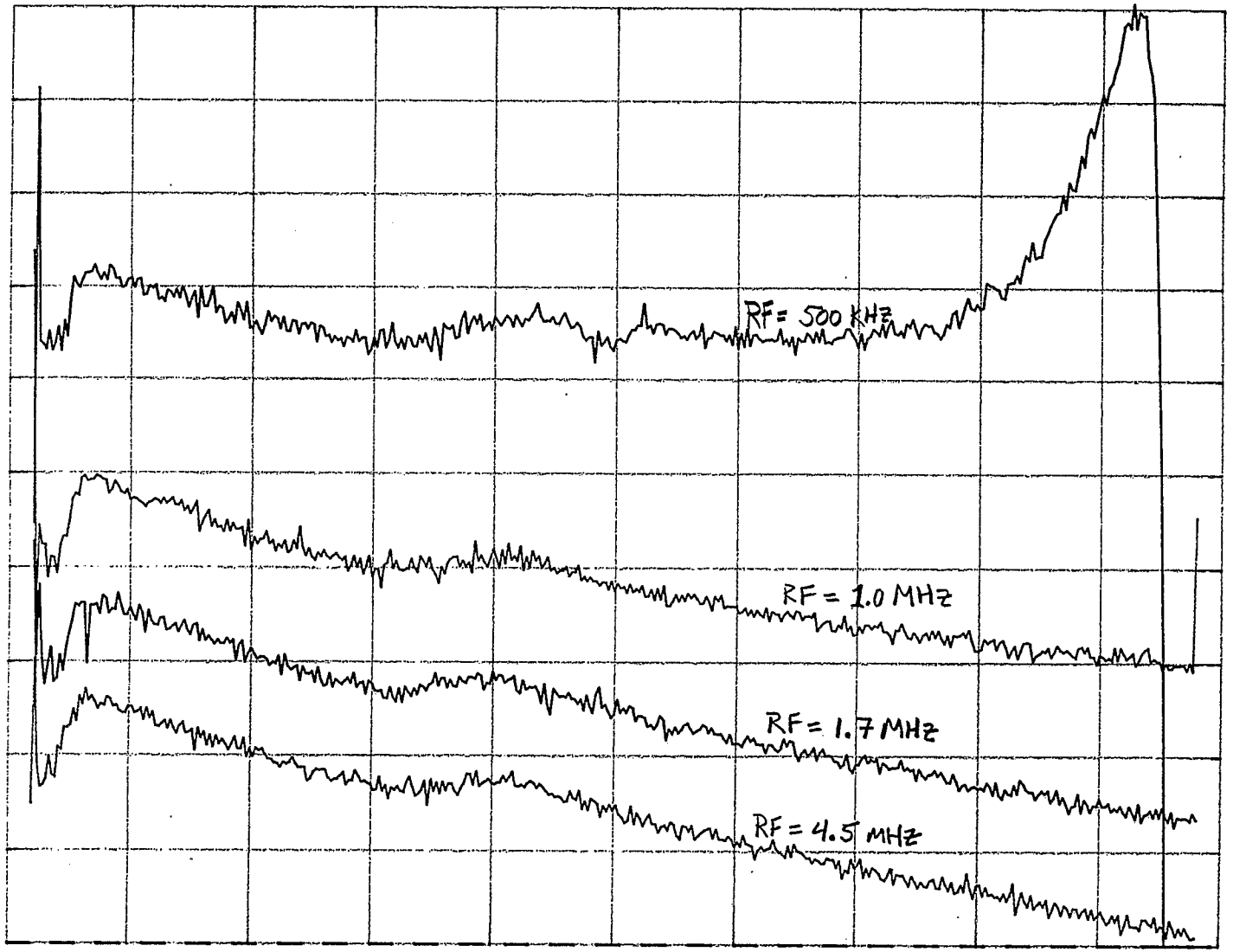

START 10.000Hz
AMPTD −5.0dBm

STOP 500 000.000Hz
DELAY APER 20.00kHz

FIG 14

TIME DELAY FOR VARIOUS RF FREQS